

Fuzzy Optimization of a Photovoltaic Pumping System: Implementation and Measurements

Hichem Othmani^{*‡}, Fares Sassi^{*}, Dhafer Mezghani^{**}, Abdelkader Mami^{**}

^{*} Laboratory of Analysis, Design and Control of Systems, National School of Engineering of Tunis University of Tunis El-Manar, The university Campus of Farhat Hached B.P. n° 94 - Rommana 1068 Tunis, Tunisia.

^{**} Department of Physics, Faculty of Sciences of Tunis, University of Tunis El-Manar, The university Campus of Farhat Hached B.P. n° 94 - Rommana 1068 Tunis, Tunisia.

[‡]Corresponding Author; Tel: +216 52 733 895,

hichem.othmani@enit.utm.tn

Received: 08.01.2017 Accepted:05.03.2017

Abstract- This paper presents a fuzzy logic optimization a photovoltaic pumping system. In this study, a photovoltaic source is connected to a three phase inverter which supplies an induction motor-pump. In addition to the induction motor pump, the hydraulic part of this system contains two communicating tanks. The effectiveness of these systems depends on the adequacy between the generated electrical energy and the quantity of the pumped water. Our designed strategy aims to exploit the maximum of the available energy whatever the climate conditions to pump water. Measurements made on the studied system demonstrate that the designed approach improves the efficiency.

Keywords Fuzzy logic controller, photovoltaic system, induction motor, centrifugal pump, scalar control, STM32F4 Board.

1. Introduction

Water is vital to all living beings on the earth. The pumping is performed for managing the water resources on different fields (surface water, groundwater, desalination, agriculture or industry). In this context, several renewable energies sources such as wind, photovoltaic and biomass are used in water pumping systems.

Using photovoltaic energy to pump water is a suitable solution for the arid and semi-arid zone. This energy has the advantage for being present and clean. In addition to that, electrical energy produced by photovoltaic effect is very attractive and is somehow a symbol of "modernity". However, conventional energies present the constraints of distance from the electrical network, the constraints of transporting fuel and periodic maintenance for diesel generators.

Several existing works in the literature have been interested on photovoltaic pumping systems. We can find works which focus on modelling the water pump system [4,5], other works are oriented to the design of these systems [13,14].

The photovoltaic pumping occurs basically in two ways depending on the nature of storage. Stations that contain batteries that store electricity generated by photovoltaic panels[2][11]. The second type contains stations that operate on the sun wire. In this case, a tank is used to store the pumped water until it is used. This later is called hydraulic storage [1].

To extract as much water with photovoltaic pumping systems that use hydraulic storage, we need to design a control strategy that takes into consideration the variation of the climate Conditions. The object of our work consists on exploiting all produced photovoltaic energy to pump, as much, water and store it in a tank. We have designed a controller that takes account of the climate condition which affects the produced energy. This controller will direct the pump to the optimal operating point through the adaptation system.

For that, we will start by modelling the studied system. Then we will present the control law that manages the system. After that, we will interpret the obtained measures. By the end, we will conclude our work.

2. Modelling of the Studied System

The adopted structure operates over the sun without batteries storage, where pumped water can be used either directly or indirectly through its storing in a tank for later use. This method, which is called hydraulic storage, is more used than electrochemical storage. Fig. 1 illustrates the studied system.

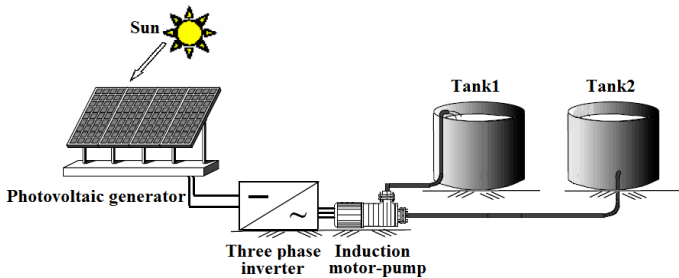


Fig. 1. Synoptic of the studied system.

2.1. Modelling of photovoltaic generator

The conversion of solar radiation into electricity by the photovoltaic process is one of the exploitation means of solar energy. Modelling PV generators can be illustrated by several ways such as graphic, empiric or analytic [2]. We choose the analytic way because it guaranties a good precision [3]. A photovoltaic panel is mathematically modelled by the following equations:

The electrical current produced by photovoltaic panel I_{pv} is given by:

$$I_{pv} = I_{ph} - I_d - I_{sh} \tag{1}$$

Electrical current of diode I_d is given by:

$$I_d = I_s \left(\exp \left(\frac{V_{pv} + R_s I_{pv}}{n C V_t} \right) - 1 \right) \tag{2}$$

V_{pv} is the photovoltaic voltage, n is the ideality factor of a diode, C is the number of cells in series per module (panel), and R_s is the series resistor.

V_t is given by:

$$V_t = \frac{K.T}{q} \tag{2}$$

q is the elementary charge in Coulomb, K is the Boltzmann constant and T is the temperature of photovoltaic cell.

I_s refers the saturation current, it highly depends on the temperature:

$$I_s = I_{rs} (T - T_{ref}) \exp \left(\frac{E_g \cdot q^2}{K.n} \left(\frac{1}{T} - \frac{1}{T_{ref}} \right) \right) \tag{4}$$

E_g is the gap energy and T_{ref} is the reference temperature of photovoltaic cell.

I_{rs} is given by

$$I_{rs} = \frac{I_{sc}}{\exp \left(\frac{q.V_{oc}}{n.K.C.T} \right)} \tag{5}$$

We note by V_{oc} the open circuit voltage of the photovoltaic panel. I_{sc} represents the short circuit electrical current of the photovoltaic panel.

The variation of I_{ph} is related to the solar radiation I_{rr} and cell temperature. The following relation proves this relation [4]:

$$I_{ph} = I_{rr} (I_{sc} + K_i (T - T_{ref})) \tag{6}$$

K_i is the coefficient of temperature.

Eventually the current of the shunt resistance I_{sh} is calculated by:

$$I_{sh} = \left(\frac{V_{pv} + R_s I_{pv}}{R_p} \right) \tag{7}$$

R_p is the shunt resistor.

Table I shows panel's data at Standard Test Condition for a Kaneka GSA 60 panel which we have used during this work.

We note by P_{max} the maximum power generated by photovoltaic panel at Standard Test Condition, V_{mpp} is the maximum voltage related to the maximum power, I_{mpp} is the maximum current related to maximum power.

Table 1. Parameters of the Photovoltaic panel KANEKA GSA60

Pmax (W)	60
Vmpp (V)	67
Impp (A)	0.9
Voc (V)	92
Isc (A)	1.19

In fact, the change of the climate conditions (irradiance and temperature) directly influences photovoltaic array. For thus, when the irradiance decreases power decreases. By the way, an increase in temperature causes a decrease on power. For thus it is so necessary to adapt these behaviors with the load. When we connect the source with the load we have to consider these changes in the power output of the PV generator, not to highlight the characteristic of the load so, that the working point would be possible.

2.2. Modelling of induction motor

The model of induction motor is obtained by applying Concordia and Park transformation. The first transformation aims to transform the three phases referential into two phases referential in order to facilitate the compute. We should mention that this transformation conserve instantaneous power. However Park transformation allows transition from alternatives magnitudes to continuous quantities.

Park transformation is defined by:

$$\begin{pmatrix} X_{sd} \\ X_{sq} \end{pmatrix} = M(\theta_s) \cdot \begin{pmatrix} X_{s\alpha} \\ X_{s\beta} \end{pmatrix} \tag{8}$$

Concordia transformation is defined by:

$$\begin{pmatrix} X_{s\alpha} \\ X_{s\beta} \end{pmatrix} = P(0) \cdot \begin{pmatrix} X_{sa} \\ X_{sb} \\ X_{sc} \end{pmatrix} \tag{9}$$

$$M(\theta_s) = \begin{bmatrix} \cos \theta_s & \sin \theta_s \\ -\sin \theta_s & \cos \theta_s \end{bmatrix}$$

$$P(0) = \sqrt{\frac{2}{3}} \begin{bmatrix} 1 & -1 & -1 \\ 0 & \frac{2}{\sqrt{3}} & \frac{2}{\sqrt{3}} \end{bmatrix} \tag{10}$$

We note by θ_s the rotation angle of the stator, precisely the angle between stator and the d-axis.

The electrical equations noted in the three phases referential (a, b, c) are: [3]

At the level of the stator:

$$U_{s(a,b,c)} = [R_s] i_{s(a,b,c)} - \dot{\phi}_{s(a,b,c)}$$

$$i_{s(a,b,c)} = \begin{bmatrix} i_{sa} \\ i_{sb} \\ i_{sc} \end{bmatrix} \quad U_{s(a,b,c)} = \begin{bmatrix} U_{sa} \\ U_{sb} \\ U_{sc} \end{bmatrix} \tag{11}$$

$$R_s = \begin{bmatrix} R_s & 0 & 0 \\ 0 & R_s & 0 \\ 0 & 0 & R_s \end{bmatrix} \quad \phi_{s(a,b,c)} = \begin{bmatrix} \phi_{sa} \\ \phi_{sb} \\ \phi_{sc} \end{bmatrix}$$

We note by R_s is resistances of Stator, $U_s(a,b,c)$ are the voltages of Stator, $i_s(a,b,c)$ are the currents of the stator and $\Phi_s(a,b,c)$: magnetic flow of the stator.

At the rotor:

$$U_{r(a,b,c)} = [R_r] i_{r(a,b,c)} - \dot{\phi}_{r(a,b,c)}$$

$$i_{r(a,b,c)} = \begin{bmatrix} i_{ra} \\ i_{rb} \\ i_{rc} \end{bmatrix} \quad U_{r(a,b,c)} = 0$$

$$R_r = \begin{bmatrix} R_r & 0 & 0 \\ 0 & R_r & 0 \\ 0 & 0 & R_r \end{bmatrix} \quad \phi_{r(a,b,c)} = \begin{bmatrix} \phi_{ra} \\ \phi_{rb} \\ \phi_{rc} \end{bmatrix} \tag{12}$$

R_r are the rotor resistances, $U_r(a,b,c)$ are the rotor voltages, $i_r(a,b,c)$ are the rotor currents and $\Phi_r(a,b,c)$: magnetic flow of the rotor.

At the stator:

$$\phi_{s(a,b,c)} = [\chi_s] i_{s(a,b,c)} - [\chi_M] i_{r(a,b,c)}$$

$$\chi_s = \begin{bmatrix} l_s & M_s & M_s \\ M_s & l_s & M_s \\ M_s & M_s & l_s \end{bmatrix} \tag{13}$$

$$\chi_M = M_{sr} \begin{bmatrix} \cos(\theta) & \cos(\theta - \frac{2\Pi}{3}) & \cos(\theta + \frac{2\Pi}{3}) \\ \cos(\theta - \frac{2\Pi}{3}) & \cos(\theta) & \cos(\theta + \frac{2\Pi}{3}) \\ \cos(\theta + \frac{2\Pi}{3}) & \cos(\theta - \frac{2\Pi}{3}) & \cos(\theta) \end{bmatrix}$$

$[\chi]$ represents inductance matrix (we note by s: stator, r: rotor and M: mutual), M_s is the mutual inductance between two stator phases, l_s is the own stator inductance, M_{sr} is the mutual inductance between stator and rotor and θ is the angle between the stator and the rotor.

At the level of the rotor:

$$\phi_{r(a,b,c)} = [\chi_M] i_{s(a,b,c)} - [\chi_r] i_{r(a,b,c)} \tag{14}$$

$$\chi_r = \begin{bmatrix} l_r & M_r & M_r \\ M_r & l_r & M_r \\ M_r & M_r & l_r \end{bmatrix}$$

We note by l_r the own rotor inductance. M_r is the mutual inductance between two rotor phases.

The mechanical equation of the induction motor is:

$$J \frac{d\Omega}{dt} = T_{em} - T_r \tag{15}$$

Ω is the real speed, T_{em} is the electromagnetic torque, T_r is the resistive torque and J is the moment of inertia.

Applying the theorem of Ferrari, we get [4]

$$T_{em} = -n_p L_M (i_{s(a,b,c)} I_{r(a,b,c)}) = n_p \frac{L_M}{L_r} (\phi_{r(a,b,c)} i_{s(a,b,c)}) \tag{16}$$

L_M is the cyclic mutual inductance, n_p is the number of pole pairs, L_r is the cyclic rotor inductance.

If we apply the Park transformation to the equations (16) we get:

$$T_{em} = n_p \frac{L_M}{L_r} (I_{sq} \Phi_{rd} - I_{sd} \Phi_{rq}) \quad (17)$$

Where I_{sd} is the stator current (d-axis), I_{sq} is the stator current (q-axis), Φ_{rd} is the rotor magnetic flow (d-axis) and Φ_{rq} is the rotor magnetic flow (q-axis).

2.3. Modelling of centrifugal pump

A centrifugal pump is a rotary machine that allows the transportation of liquid inside the hydraulic network. This machine is characterised by geometric height, level of elevation (Z) and pressure (p). The calculation of centrifugal pumps is effected by dimensional analysis and by Euler's theorem.

Q is the flow provided by a centrifugal pump as the volume discharged during the time unit.

H_{pompe} is the energy supplied by the pump at the weight unit of the flowing liquid through it. This height depends on the flow rate. It is represented by the characteristic curve $H_{pompe} = f(Q)$ for constant speed given by the manufacturer. [2] [4]

$$H_{pompe} = b_0 \Omega_m^2 + b_1 \Omega_m Q + b_2 Q^2 \quad (18)$$

The coefficients b_0 , b_1 and b_2 are based on the internal geometry of the pump and independent of the speed of rotation. They can be determined experimentally by meeting three points of the H_{pompe} characteristic.

The centrifugal pump has a characteristic of the resistant torque T_r (Ω) proportional to the square of its rotational speed Ω_m which is given by the following equation aerodynamic [1]:

$$T_r(\Omega) = C_2 \Omega_m^2 \quad (19)$$

C_2 is the torque constant of the pump.

The useful mechanical power P_m supplied by the drive motor to the pump is:

$$P_m = C_2 \Omega_m^3 \quad (20)$$

The mechanical losses on the level of the shaft of the pump are represented by T_{fv} (Ω), it is described by the following expression in which C_1 is the viscous friction coefficient.

$$T_{fv} = C_1 \Omega_m \quad (21)$$

Couples presented above is added acceleration torque $J.d\Omega_m / dt$, where J is the total inertia of the mechanical system and t is time, thus electromagnetic torque is described by the following expression:

$$T_{em} = C_2 \Omega_m^2 + C_1 \Omega_m + J \frac{d\Omega_m}{dt} \quad (22)$$

To determine the operating point we must begin with the structure below

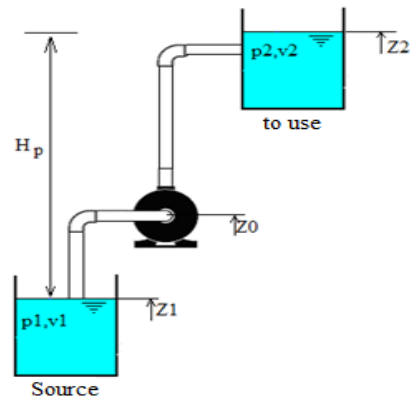


Fig. 2. Synoptic of Hydraulic system.

With the generalized Bernoulli relationship, we can explain the manometric height H_{pompe} of the pump through:

$$\left(\frac{v_1^2}{2g} + \frac{p_1}{\rho g} + Z_1 \right) + H_{pompe} = \left(\frac{v_2^2}{2g} + \frac{p_2}{\rho g} + Z_2 \right) + \sum_i h_i \quad (23)$$

H_p is the total geometric height, p_1 is the inlet pressure, p_2 is the outlet pressure, v_1 is the suction velocity, v_2 is the discharge speed, $\frac{p}{\rho g}$ pressure height, $\frac{v^2}{2g}$ is the dynamic height, Z is the position height and $\sum h_i$ are the losses in the suction and discharge.

When we neglect the terms of speed and we assume $p_1 = p_2$, the term of the height of the hydraulic system is given by:

$$H_{circuit} = H_p + \Psi Q^2 \quad (24)$$

The operating point of the installation is the intersection between $H_{pompe}(Q)$ at constant speed and $H_{circuit}(Q)$ (defined by the flow rate Q on which the pump is automatically adjusted).

This intersection is expressed by the following relationship:

$$b_0 \Omega_m^2 + b_1 \Omega_m Q + b_2 Q^2 = H_p + \Psi Q^2 \quad (25)$$

$$(b_2 - \Psi) Q^2 + b_1 \Omega_m Q + (b_0 \Omega_m^2 - H_p) = 0 \quad (26)$$

This is a second degree equation Q , its resolution is used to determine the water flow generated by the pump for a given speed of rotation. This pump begins to generate a flow rate from a minimum speed defined by [6]:

$$\Omega_{min} = \sqrt{\frac{-4(b_2 - X)H_p}{b_1^2 - 4(b_2 - \Psi)b_0}} \quad (27)$$

We will discuss three possible cases following the recorded value of the speed:

If $\Omega_m < \Omega_{min}$ there is no flow generated by the pump, that's means:

$$\Omega_{\min} = \sqrt{\frac{-4(b_2 - X)H_p}{b_1^2 - 4(b_2 - \Psi)b_0}} \quad (28)$$

If $\Omega_m = \Omega_{\min}$ the pump starts delivering water:

$$Q = Q_{\min} = \frac{b_1 \Omega_{\min}}{2(b_2 - \Psi)} \quad (29)$$

If $\Omega_m > \Omega_{\min}$ expression rate is given by:

$$Q = \frac{-b_1 \Omega_m - \sqrt{(b_1 \Omega_m)^2 - 4(b_2 - \Psi)(b_0 \Omega_m^2 - H_p)}}{2(b_2 - \Psi)} \quad (30)$$

In the case where tanks are constantly connected to each other and on the same plane (case of our application), the rule will be:

$$Q = \left(\frac{-b_1 - \sqrt{b_1^2 - 4b_0^2(b_2 - X)}}{2(b_2 - X)} \right) \Omega_m = \left(\frac{Q_{nom}}{\Omega_{nom}} \right) \Omega_m \quad (31)$$

Electrical specifications of induction motor-Pump are described on table II.

Table 2. Specifications of EBARA induction motor-pump.

Nominal output power (W)	370
Nominal electrical power(W)	550
Max Flow Rate (l/min)	35.60.9
Max head (m)	7
Statoric resistor(Ω)	24.6
Rotoric resistor (Ω)	16.1
Mutual self(H)	1.46
Rotoric self (H)	1.48
Statoric self(H)	1.49
C1(kg.m ² .s ⁻¹)	1.75. 10 ⁻³
C2(Kg.m ⁴ .s ⁻²)	7.5. 10 ⁻⁶
J(Kg.m ⁻¹)	6.5. 10 ⁻³
b ₀ (min ² .m.tr ⁻²)	4.52. 10 ⁻⁴
b ₁ (m.min ² .tr ⁻¹ .L ⁻¹)	-1.966.10 ⁻³
b ₂ (min ² .m.L ⁻²)	-0.012
Ψ(min ² .m.L ⁻²)	4.0816 10 ⁻³

3. Control law

Using MPPT control does not guarantee the maximum system efficiency. For thus, and in order to improve the robustness of the control strategy against the variations of climate condition, we design a fuzzy controller which can find the optimal speed related to each irradiance and temperature value. Figure 10 illustrate the principle of operation of the fuzzy controller

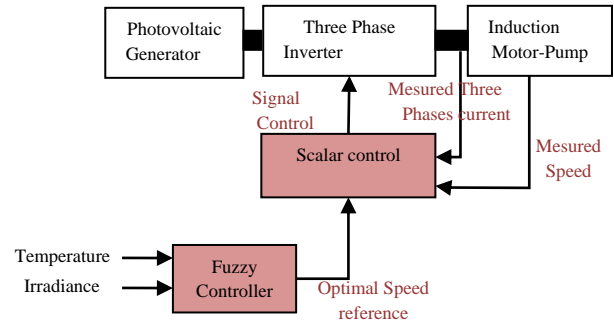


Fig. 3. Control law structure

3.1. Scalar control

We have used in this work the scalar control. This strategy is based on the equivalent circuit per phase of the induction motor illustrated below:

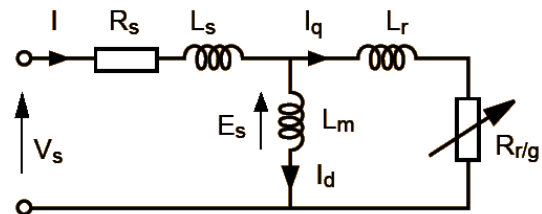


Fig. 4. Equivalent circuit per phase of the induction motor.

The magnetic flow is created by the current flowing through the magnetizing inductance L_m . The optimum performance of the induction motor is obtained if the magnetizing current is maintained substantially constant over the entire speed range. The magnetizing current can be calculated by the following expression:

$$I_d = \frac{E_s}{L_m \omega} \quad (32)$$

$$E_s = V_s - (R_s + jL_s \omega) I \quad (33)$$

$$I_d = \frac{V_s}{\omega L_m} \quad (34)$$

The magnetizing current can be maintained constant by keeping constant V_s/f . However, we have to be in mind that at low frequencies and voltages, the term $(R_s + L_s \omega)I$ will be significant and a result the maintain of V_s/f constant will be not enough. [5]

There are various profiles of control laws V_s/f which allows the adaptation of different types of loads encountered [5]. We choose the quadratic profile in which the resisting torque exerted by the centrifugal pump depends on the square of the speed. Therefore we can, and without any effects, reduce the motor flux. As result, the supply voltage of the motor at a frequency will be lower than the nominal frequency.

3.2. Fuzzy logic controller

Recently, fuzzy logic controller (FLC) is one of the artificial intelligence methods which offering high performance, and can control complex systems intuitively. One of the advantages of this controller is its ability to understand the problems of nonlinearity and exhibit robust performance without any undesirable effect.

Designing Fuzzy Logic controller proceeds compulsory through four steps: fuzzification, knowledge base, inference engine, and a defuzzification. These four steps are summarized in Fig. 5. The principle of the first step is transforming numerical data inputs to linguistic terms which are understood by fuzzy controller. Knowledge base is the data base of the controller which offers necessary information for all components of the fuzzy controller [13-15]. The fuzzy inference engine is the make-decision step. Finally, defuzzification is the reverse step of fuzzification.

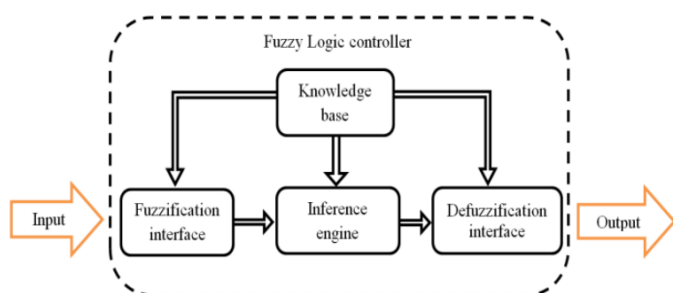


Fig. 5. Basic configuration of a fuzzy logic controller.

The fuzzy logic controller measures climatic conditions and then set optimal frequency.

Using Matlab toolbox “fuzzy logic toolbox”, shown in Fig. 6, the designed fuzzy logic controller contain two inputs (Irradiance and Temperature) and one output which frequency is.

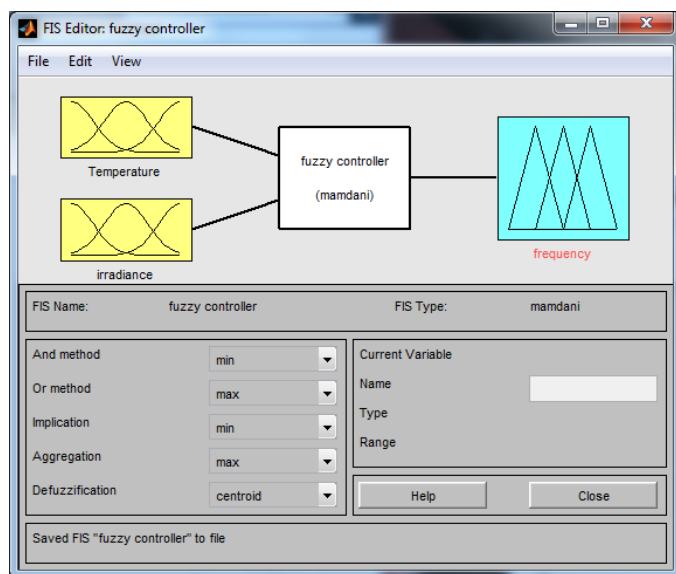


Fig. 6. Graphical interface of the fuzzy logic toolbox.

Table 3. Related proprieties of the fuzzy logic controller

Type of controller	Mamdani
And method	Min
Or method	Max
Implication	Min
Deffuzification	Centroid

We have opted for triangular and trapezoidal functions for variables inputs (Fig.11, 12 and 13). They allow for an easy implementation and fuzzification step. In addition to that, they require little computation time when evaluated in real time.

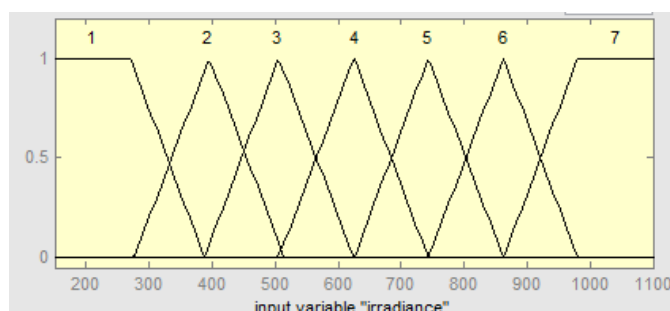


Fig. 7. Membership functions of Irradiance.

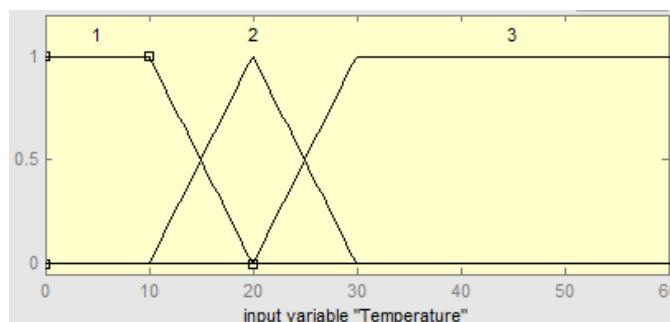


Fig. 8. Membership functions of Temperature.

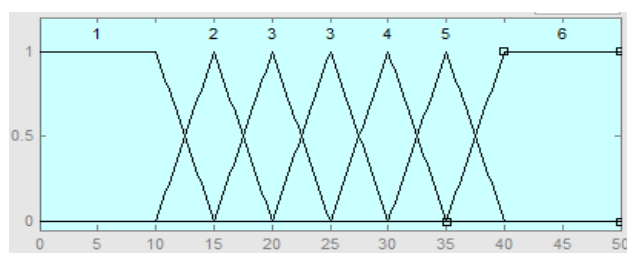


Fig. 9. Membership functions of Frequency.

We explain the operation of fuzzy controller by the three yellow rules as an example.

If Irradiance is 1, and Temperature 1, then fuzzy controller should set frequency at 2. That’s mean; when the irradiance is very weak and the temperature is cold the frequency should be small.

If Irradiance and Temperature are medium, then fuzzy controller should set frequency at medium value.

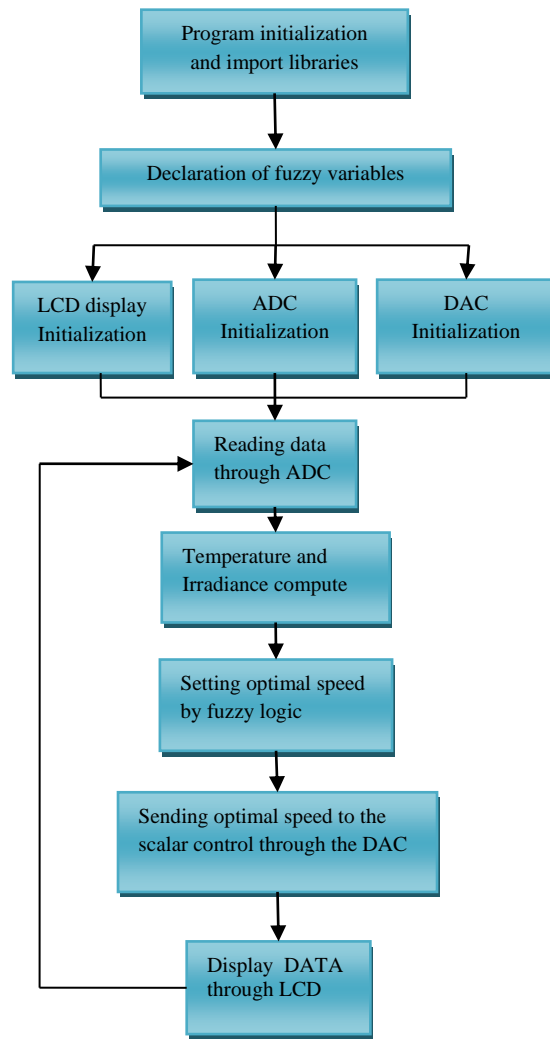
In other case if we have a high irradiance and a high temperature, the fuzzy controller should set a high frequency. It should be noted that the exact values of the controller

constants were found after performing experiences on the studied system which helped us to define each membership functions.

Table 4. Fuzzy inference rules

Rule N°	Irradiance	Temperature	Frequency
1	1	1	2
2	2	1	3
3	3	1	4
4	4	1	5
5	5	1	6
6	6	1	7
7	7	1	7
8	1	2	1
9	2	2	2
10	3	2	3
11	4	2	4
12	5	2	5
13	6	2	6
14	7	2	7
15	1	3	1
16	2	3	1
17	3	3	2
18	4	3	3
19	5	3	4
20	6	3	5
21	7	3	6

The diagram of implemented algorithm is given by Fig.10.



4. Results and discussion

In order to validate the designed strategy, we have implemented the fuzzy controller on STM32F4 Board.

Fig. 10. Diagram of the implemented algorithm.

Under Cube-Mx software, we present the used peripherals on STM32F4 Board (fig.11.) with green color.

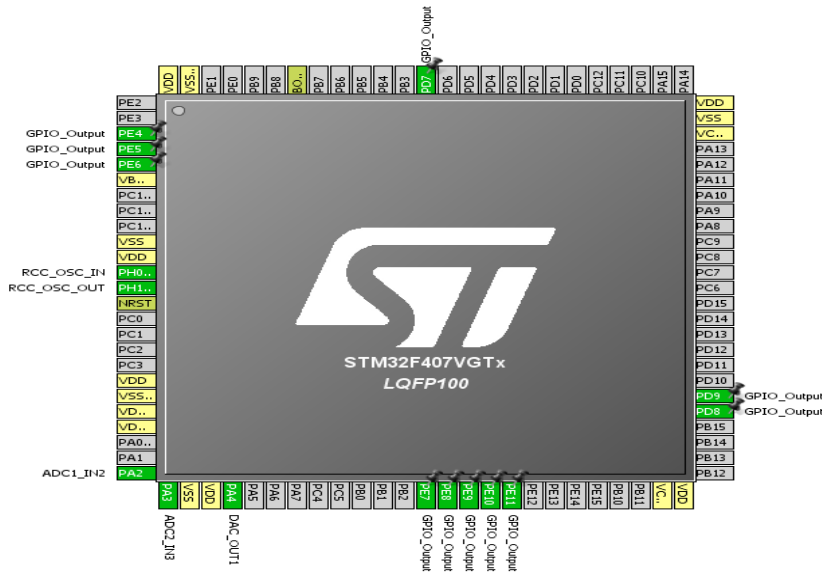


Fig. 11. The used peripherals on STM32F4 Board.

The two ADC (Analog Digital Converter) pins are used for reading climatic conditions. DAC (Digital Analog Converter) pin is used to transmit optimal frequency to DV51 inverter which includes the scalar control. The other GPIO-Output ensure the communication with LCD display.

Fig.12. shows the connection between the different elements of the studied system. Climatic conditions (irradiance and temperature) are acquired through a photo-resistance and LM35 sensor. The STM32 F4 Board set the optimal speed which transferred to the inverter. The DV51 is a three phase inverter which includes a scalar control.

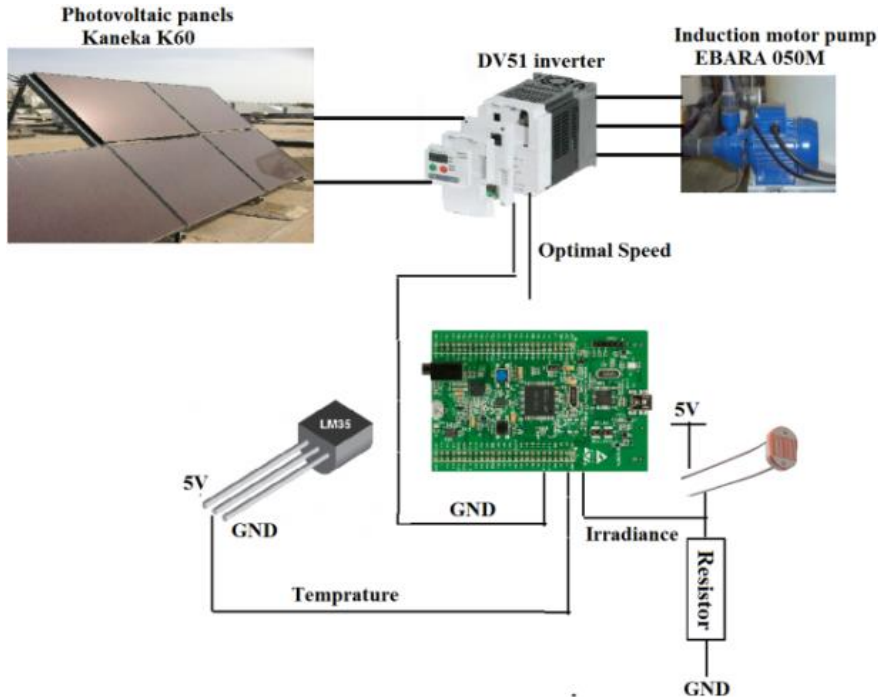


Fig. 12. Connection of STM32F4 Board to the studied system.

Induction motor-pump (element2) transfer water from left tank to right tank (element 6) as shown in fig.13. The hydraulic system includes different sensors: pressure (element 7), and flow (element 5). The pipe (element 3) is connected by a valve assembly (element 4). For this installation, we have to combine four photovoltaic panels in series.

Fig.14. shows connection between LCD Display and STM32F4 Board. Figure.15. illustrates data display through LCD in real Time.



Fig. 13. Real picture of the studied System.



Fig. 14. Connection between LCD Display and STM32F4 Board.



Fig. 15. LCD data displays.

After the controller was designed and implemented, we carried out such measures during two days: October 03rd 2016 and October 23th 2016.

Fig. 16 and 17 present the behavior of the irradiance and of the temperature during these two days.

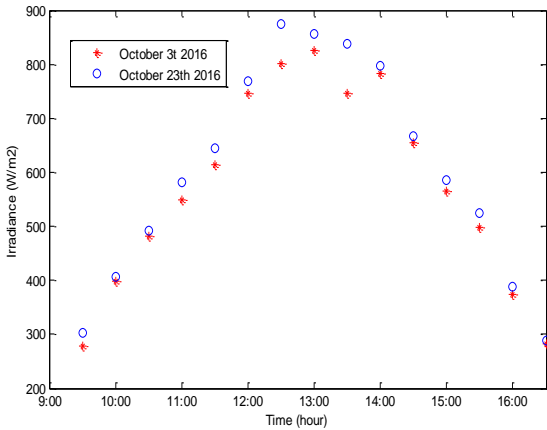


Fig. 16. Measure of Irradiance.

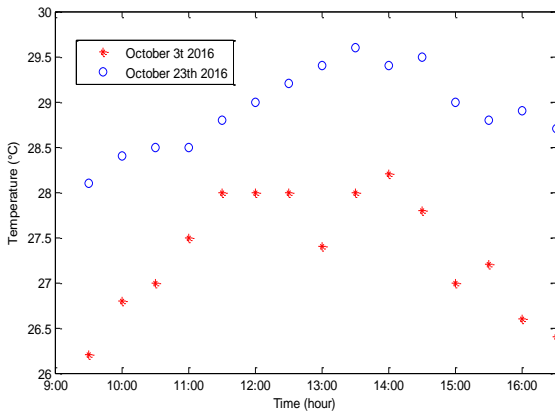


Fig. 17. Measure of Temperature.

The behavior of the climatic condition have allowed us to achieve results as shown in Fig. 18, 19, 20 and 21 that are related to the flow rate and Power of each element.

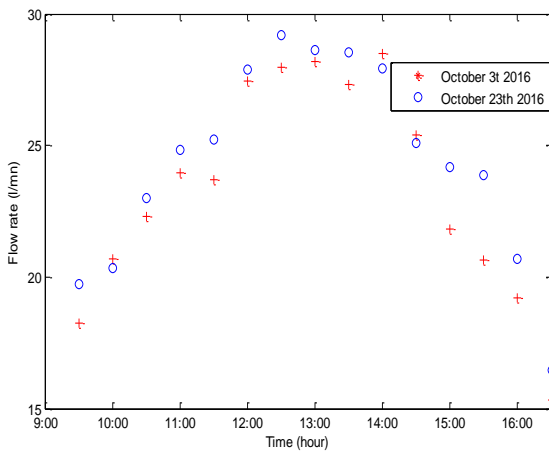


Fig. 18. Measure of the flow rate.

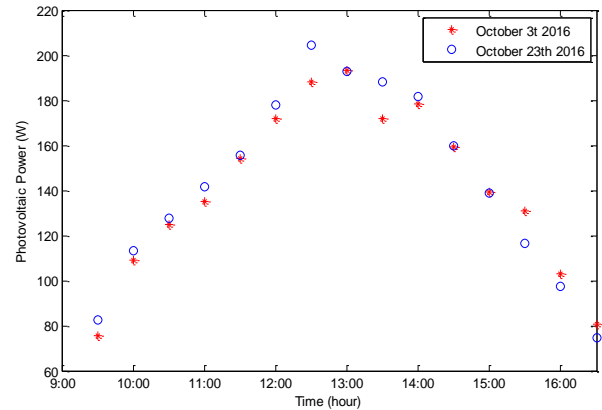


Fig. 19. Photovoltaic power behaviour.

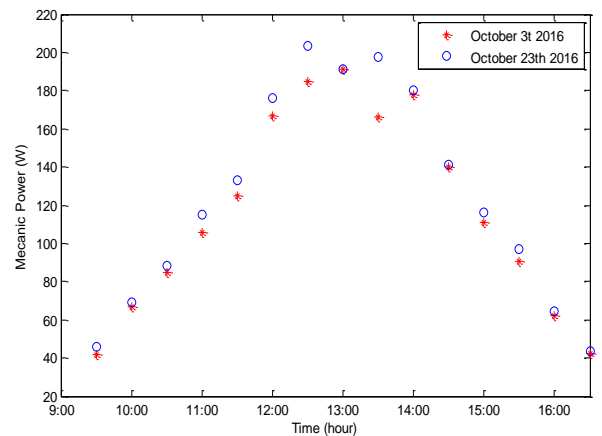


Fig. 20. Mechanical power behaviour.

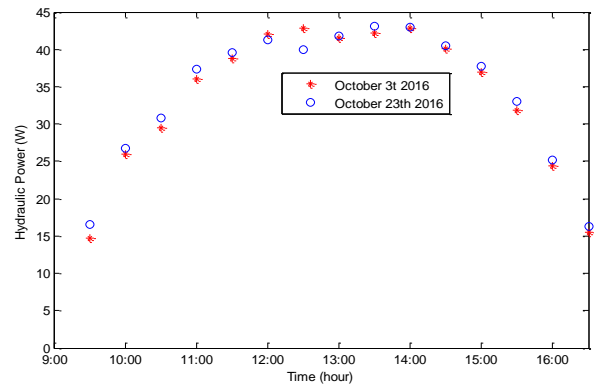


Fig. 21. Hydraulic power behaviour.

As we can see, the use of fuzzy logic controller has guaranteed an optimal photovoltaic power against the climatic conditions variations during the recorded days. It is clear that the produced power absolutely depends on irradiance. Our fuzzy technique has generate an optimal frequency that kept increasing function is almostly with the irradiance. We have seen that temperature change is less important on the system behavior. This configuration allows water to be pumped with a flow rate that ranges between 18 and 29 liter per minute (fig.18.). The optimum quantity of pumped water is obtained for a nominal speed θ_a is delivered at a mechanical power which is around 211W (fig.20).

5. Conclusion

The recorded measurements show clearly the robustness of the designed fuzzy controller against climatic condition changes have allowed transferring maximum efficiency to the pump. These results appear satisfactory. This technique was validate by experiment results.

References

- [1] A. Khiareddine, C. Ben Salah, and M. F. Mimouni, "Power management of a photovoltaic/battery pumping system in agricultural experiment station," *Solar Energy*, vol. 112, pp. 319–338, 2015.
- [2] A Betka, A. Moussi, "Performance optimization of a photovoltaic induction motor pumping system", *Renewable Energy*, Vol 29, pp 2167–2181, 2004.
- [3] A. Braustein and A. Kornfeld, "Analysis of solar powered electric water pumps", *solar energy*, Vol 27, No 3 pp 235-240, 1981.
- [4] A.L. Nemmour, F. Mehazzem, A. Khezzar, M. Hacil, L. Louze, R. Abdessemed, "Nonlinear control of induction motor based on the combined multi-scalar machine model and backstepping approach", *Industrial Electronics. (IECON) 35th Annual Conference of IEEE*, Pp. 4203-4208, 2009.
- [5] D. Weiner and A. Levinsio, "Water pumping optimal operation, *Electrical machines and power systems*", Vol 24, No 3, pp 277-288, 1966.
- [6] D. Mezghanni , R.Andoulsi, A, Mami and G. Dauphin-Tanguy , "Bond graph modelling of a photovoltaic system feeding an induction motor-pump", *Simulation Modelling Practice and Theory* voln°15, pp. 1224–1238, 2007.
- [7] D.Ounnas, M.Ramdani, S.Chenikher, and T.Boukthir, "A Fuzzy Tracking Control Design Strategy for Wind Energy Conversion System". *International Conference on Renewable Energy Research and Applications*, Palermo, Italy, 22-25 Nov 2015.
- [8] E.H. Mamdani, "Application of fuzzy algorithms for control of simple dynamic plant. *Electrical Engineers*", *Proceedings of the Institution*, Vol.121, no. 12, pp. 1585- 1588, 1974.
- [9] H.A. Al-Waeli, M.K. El-Din, A.H. K.Al-Kabi, A.Al-Mamari, H. Kazem and M.T. Chaichan "Optimum Design and Evaluation of a Solar Water Pumping System for rural Areas", *International Journal of Renewable Energy Research*, Vol. 7, No. 1, 2017.
- [10] H.Ying, "Conditions for general Mamdani fuzzy controllers to be nonlinear", *NAFIPS Annu. Meeting*, pp. 201–203, 2002.
- [11] I.Ouachani, A.Rabhi, B.Tidhaf, S.Zouggar and A.Elhajjaji, "Optimasation and control for a photovoltaic system". *International Conference on Renewable Energy Research and Applications*, Madrid, Spain, 20-23 October 2013.
- [12] I. Yahyaoui, M.Chaabene and Fernando Tadeo "An Algorithm for Sizing Photovoltaic pumping system for Tomatoes Irrigation". *International Conference on Renewable Energy Research and Applications*, Madrid, Spain, 20-23 October 2013.
- [13] J.M. Caro, J. Bonal, " *Entraînements Electriques à Vitesse Variable*", vol. 1, Lavoisier, 1997.
- [14] J. Lee, "On methods for improving performance of PI-type fuzzy logic controllers", *IEEE Trans. Fuzzy Syst*, vol. 1, no. 4, pp. 298–301, 1993.
- [15] L. Zadeh, *Fuzzy Sets. Information and Control*, vol. 8, pp. 338-353, 1965.
- [16] O. Safarini, "Developping Digital control system Centrifugel pump unit", *International Journal of Advanced Computer Science and Applications*, Vol. 2, No. 7, 2011.
- [17] M.I. Chergui, and M.O Benaissa, " Strategy photovoltaic pumping system in scattered area". *International Conference on Renewable Energy Research and Applications*, Palermo, Italy, 22-25 Nov 2015.
- [18] M. Ellouze, R. Gamoudi, A. Mami, "Sliding Mode Control Applied to a Photovoltaic Water-Pumping System", *International Journal of Physical Sciences* Vol. 5(4), pp. 334-344, April 2010. ISSN 1992 - 1950 © 2010.
- [19] N.A.Elsombaty, M.A.Enany and M.M.Gamil "Sliding Soft Computing Modling of a directly Coupled PV Water Pumping System ", *International Journal of Renewable Energy Research*, Vol. 6, No. 1, 2016.
- [20] P.Vas, "Artificial Intelligence based Electrical machines and Drives Application of Fuzzy, Neural", *Fuzzy-neural, and Genetic-algorithm-based Techniques*, ISBN 978-0-19-859397-3, 1999.
- [21] P. Borne, G. Dauphin-Tanguy, J.P. Richard, F. Rotella, I. Zambettakis, "Analyse et régulation des processus industriels ", *Méthodes et pratiques de l'ingénieur*, éditions Techni, Paris, 1993.
- [22] S.Karim, S.Gdaim, A.Mtibaa and M.F.Mimouni "FPGA contribution in photovoltaic pumping systems: Models of MPPT and DTC-SVM Algorithms ", *International Journal of Renewable Energy Research*, Vol. 6, No. 3, 2016.

- [23] T. Amel, A. Moussi, T. Nadjiba, "Design of ANFIS Estimator of Permanent Magnet Brushless DC Motor Position for PV Pumping System". International Journal of Advanced Computer Science and Applications, Vol. 6, No. 10, 2015.
- [24] Y. Tang, L. Xu, "Fuzzy logic application for intelligent control of a variable speed drive". IEEE-PES Winter Meet, 1994.
- [25] Y.Soufi, M. Bechouat, S.Kahla, and K. Bouallegue, "Optimisation Maximum power point tracking using fuzzy logic control for photovoltaic system". International Conference on Renewable Energy Research and Applications, Milwaukee, USA 19-22 Oct 2014